

Provided by the author(s) and University of Galway in accordance with publisher policies. Please cite the published version when available.

Title	The natural bile acid surfactant sodium taurocholate (NaTC) as a coformer in coamorphous systems: Enhanced physical stability and dissolution behavior of coamorphous drug-NaTc systems
Author(s)	Gniado, Katarzyna; MacFhionnghaile, Pól; McArdle, Patrick; Erxleben, Andrea
Publication Date	2018-10-28
Publication Information	Gniado, Katarzyna, MacFhionnghaile, Pól, McArdle, Patrick, & Erxleben, Andrea. (2018). The natural bile acid surfactant sodium taurocholate (NaTC) as a coformer in coamorphous systems: Enhanced physical stability and dissolution behavior of coamorphous drug-NaTc systems. <i>International Journal of Pharmaceutics</i> , 535(1), 132-139. doi: https://doi.org/10.1016/j.ijpharm.2017.10.049
Publisher	Elsevier
Link to publisher's version	https://doi.org/10.1016/j.ijpharm.2017.10.049
Item record	http://hdl.handle.net/10379/7192
DOI	http://dx.doi.org/10.1016/j.ijpharm.2017.10.049

Downloaded 2024-04-17T22:59:51Z

Some rights reserved. For more information, please see the item record link above.



The Natural Bile Acid Surfactant Sodium Taurocholate (NaTC) as a Coformer in Coamorphous Systems: Enhanced Physical Stability and Dissolution Behavior of Coamorphous Drug-NaTC Systems

Katarzyna Gniado, Pól MacFhionnngaile, Patrick McArdle* and Andrea Erxleben*

School of Chemistry, National University of Ireland, Galway, Ireland

Abstract

The amorphization of 18 different drugs on milling with one mole equivalent sodium taurocholate (NaTC) was investigated. In all cases the X-ray powder pattern showed an amorphous halo after milling at room temperature or after cryomilling and 14 of the 18 coamorphous drug-NaTC systems were physically stable for between one to eleven months under ambient storage conditions. In three cases, namely carbamazepine-NaTC, indomethacin-NaTC and mefenamic acid-NaTC, significant dissolution advantages over the crystalline drugs were observed, both for the freshly prepared samples and after storage for seven months. To understand the increased physical stability, infrared-, near-infrared and Raman spectroscopic studies were carried out. The effectiveness of NaTC as a coformer in a diverse range of coamorphous systems is attributed to its awkward molecular shape that hampers recrystallization and phase separation and its propensity to form a range of similar, yet different drug-coformer hydrogen bonding arrangements.

Keywords

Amorphous; Crystallization inhibition; Dissolution studies; Spectroscopy

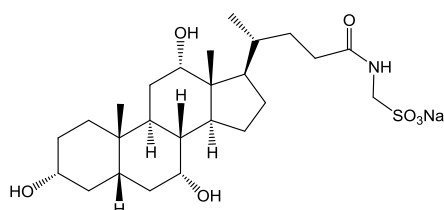
1. Introduction

Amorphization increases the apparent solubility and can lead to an improved dissolution behavior and bioavailability of poorly soluble drugs. However, the enhanced solubility of the high-energy, amorphous form comes at the cost of low thermodynamic stability and the true

solubility advantage is often lost due to rapid recrystallization on contact with the dissolution medium or even during storage. Consequently, a range of formulation strategies for amorphous drugs are being explored (Grohgan et al., 2014). One of the most widely investigated amorphous formulations are polymeric amorphous solid dispersions (ASDs) in which the drug molecules are intimately mixed with the polymer molecules of an excipient and the amorphous phase is stabilized by drug-polymer intermolecular interactions such as hydrogen bonding. Soprona[®], Novir[®] and Kaletra[®] are examples for drugs that are currently marketed as polymeric amorphous solid dispersions (Teja et al., 2013). However, often large amounts of polymer are needed due to poor drug-polymer miscibility, leading to large tablet sizes and limiting the use of ASDs for high dosage drugs. Furthermore, issues with scale-up often pose challenges for the final dosage form development. The hygroscopic nature of some polymers can also facilitate phase transformation during processing or storage (Kaushal et al., 2004). The latter has led to polymer ASD products having had to be recalled by the FDA (Guo et al., 2013). More recently, so-called coamorphous systems have emerged as promising formulations. In contrast to polymeric ASDs, coamorphous systems are stoichiometric binary systems of two compatible drugs (Yamura et al., 1996 & 2000; Chieng et al., 2009; Alessø et al., 2009; Löbmann et al., 2011 & 2012) or of a drug and a pharmaceutically acceptable small-molecule coformer (Lu and Zografi, 1998; Masuda et al., 2012; Hoppu et al., 2007 & 2009). Coformers that have been successfully applied to stabilize an amorphous drug include saccharin (Gao et al., 2013), nicotinamide (Shayanfar, 2013), carboxylic acids (Lu and Zografi, 1998; Masuda et al., 2012; Hoppu et al., 2007 & 2009; Ali et al., 2015; Han et al., 2016; Hu et al., 2014) and sugars (Descamps et al., 2007). In particular, amino acids capable of forming charge-assisted hydrogen bonds have been widely studied (Löbmann et al., 2013; Jensen et al., 2014, 2015 & 2016; Laitinen et al., 2014; Lenz et al., 2015; Huang et al., 2016; Craye et al., 2015). On the other hand, an increase in the physical stability was observed for coamorphous simvastatin-glipizide, even though there was no evidence for intermolecular interactions, suggesting that molecular level mixing may be sufficient to stabilize the amorphous phase (Löbmann et al., 2012).

It has been shown that the dissolution profile and bioavailability of ASDs can be significantly improved by using polymers with surface activity or mixtures of a polymer and a surfactant (Chauhan et al., 2005; Won et al., 2005). We have recently applied the natural bile acid surfactant sodium taurocholate (NaTC, Scheme 1) as a small-molecule coformer for a sulfa drug coamorphous system and demonstrated that coamorphous sulfamerazine-NaTC displays

a significantly enhanced dissolution rate along with a high stability towards recrystallization (Gniado et al., 2016). We have now extended our coamorphization studies with NaTC to a wide range of active pharmaceutical ingredients (APIs). In particular, we have focused our attention on the mechanism of the increased stability of APIs amorphized by co-milling with NaTC.



Scheme 1. Molecular structure of NaTC.

2. Materials and methods

2.1 Materials

Sodium taurocholate [Lot number HE53M], acyclovir (>98 %), allopurinol (>98 %), carbamazepine (>97 %), ciprofloxacin (>98 %), indomethacin (>98 %), ibuprofen (>98 %), 6-mercaptopurine (>98 %), nifedipine (>98 %), norfloxacin (>98 %) and paracetamol (>98 %) were purchased from Tokyo Chemical Industry (TCI Europe, Zwijndrecht, Belgium). Benzamidine (>98 %), mefenamic acid (>98 %), sulfamerazine (≥ 99 %) and sulfathiazole (≥ 98 %) were obtained from Sigma Aldrich (St. Louis, Missouri). Diflunisal was purchased from Baoji Guokang Technology Co., Ltd., China. Naproxen was received as a gift from Roche Ireland Ltd. All chemicals were used as received.

2.2. Methods

2.2.1. Preparation of amorphous API-NaTC mixtures

Acyclovir-NaTC, allopurinol-NaTC, amoxicillin trihydrate-NaTC, benzamidine-NaTC, carbamazepine-NaTC, ciprofloxacin-NaTC, ibuprofen-NaTC, indomethacin-NaTC, naproxen-NaTC, nifedipine-NaTC, norfloxacin-NaTC, paracetamol-NaTC, quinine-NaTC and sulfamerazine-NaTC: The API and NaTC were mixed in a 1:1 molar ratio (1.0 g in total) and the mixture was milled for 180 min at 25 Hz in a 25-mL stainless steel jar containing one

15-mm stainless steel ball using an oscillatory ball mill (Mixer Mill MM400; Retsch GmbH, Haan, Germany). A break of 15 min was taken after 30 min of milling to avoid overheating of the sample. Immediately after milling, the sample was analyzed by X-ray powder diffraction.

Amorphous indomethacin, carbamazepine, diflunisal-NaTC, 6-mercaptopurine-NaTC, mefenamic acid-NaTC, naproxen-NaTC and sulfathiazole-NaTC: The milling jars containing 1.0 g of an equimolar mixture of the API and NaTC or 1.0 g of the API were sealed and immersed in liquid nitrogen for 3 min before milling for 120 min. Every 7.5 min, the milling jars were re-cooled with liquid nitrogen for 2 min. The average sample temperature measured at 7.5 min intervals was -10 ± 2 °C. Immediately after milling, the sample was analyzed by X-ray powder diffraction.

2.2.2. Stability testing

All samples were kept at room temperature (22 ± 2 °C, 60 % relative humidity), in sealed vials. X-ray powder diffraction was used to monitor the recrystallization of the amorphous phases.

2.2.3. Dissolution testing

Dissolution studies were carried out under sink conditions using a VanKel Variant Agilent VK7000 (Agilent Technologies, USA) dissolution test system (USP Type II, paddle) with a Distek TCS 0200C thermocirculator (Distek Inc., USA). Weighed out powder samples (Table S1) were placed in 900 mL of 0.1 M phosphate buffer (pH 6.8, 37°C) and stirred at 150 rpm. 2.5 mL aliquots were withdrawn at 2, 5, 10, 15, 25, 30, 45 and 60 min and immediately replaced with 2.5 mL of fresh dissolution medium. The withdrawn samples were filtered through a 0.20 µm cellulose acetate filter (GVS Filter Technology UK Ltd.) and analyzed the same day using UV/Vis spectroscopy. All dissolution experiments were carried out in triplicate. The amount of the dissolved API was determined by UV/Vis spectroscopy using quartz cuvettes on a Varian Cary 50 Scan Spectrophotometer (Santa Clara, CA, USA). Reference spectra were recorded for the buffer solution and the buffer solution containing NaTC, in the range from 200 to 500 nm, in order to exclude any interference with the API absorption in this range. The wavelengths used to determine the API concentrations are given in Table S1. Standard solutions of all APIs were prepared in phosphate buffer (0.1 M, pH 6.8). The resulting calibration curves were linear in the relevant concentration ranges.

2.2.4. X-ray powder diffraction (XRPD)

XRPD patterns were recorded on an Inel Equinox 3000 powder diffractometer (Artenay, France), fitted with a curved position sensitive detector calibrated using Y₂O₃. Data were collected between 5 and 90 ° (2 θ) using Cu K α radiation (λ = 1.54178 Å, 35 kV, 25 mA).

2.2.5. Attenuated total reflectance infrared spectroscopy (ATR-IR)

ATR-IR spectra were recorded with a PerkinElmer Spectrum 400 (FT-IR/FT-NIR spectrometer, Waltham, Massachusetts) equipped with a DATR 1 bounce Diamond/ZnSe Universal ATR sampling accessory. Spectra were measured in the range from 4000 to 650 cm⁻¹ with 32 accumulations and a resolution of 4 cm⁻¹.

Standard normal variate (SNV) transformation was used to normalize the spectra, reducing baseline offset and increasing signal to noise ratio:

$$x_{i,mod} = \frac{x_i - (\text{mean } X_i)}{\sigma X_i}$$

This allows equivalent analysis between samples regardless of spectral variations resulting from changes in particle size and pressure force during sampling. Calculated spectra of equimolar physical mixtures of APIs and NaTC were generated from the mean of SNV pre-treated spectra of the respective API and NaTC.

2.2.6. Near-infrared spectroscopy

Near-infrared (NIR) spectra were collected in glass vials (15 × 45 mm²) on a PerkinElmer Spectrum One (Waltham, Massachusetts) fitted with an NIR reflectance attachment. Spectra were collected with interleaved scans in the 10,000–4000 cm⁻¹ range (8 cm⁻¹ resolution, 32 co-added scans). Again, SNV pre-treatment was applied to the spectra and simulated spectra of physical mixtures were calculated as described above.

2.2.7. Raman microscopy

Raman microscopy was conducted using a Reinshaw inVia confocal microscope with a x50 optical lens controlled using the WiRE 3.4 software. Powdered samples were lightly dispersed manually on a glass slide using a spatula. Individual particles were focused and

selected using a XYZ sample stage. Spectra were collected from 665.14 to 1777.34 cm^{-1} using 600/cm grating (785 nm laser at 10% power; 3 acquisitions, 3 s exposure time).

2.2.8. Scanning electron microscopy (SEM)

SEM images were obtained using a Hitachi S2600N Variable Pressure Scanning Electron Microscope with a backscatter BSE resolution of 20 nm at 25 kV, X 903 magnification, with an accelerating voltage of 5 kV, an emission current of 10000 nA at a working distance of 13.5 mm.

2.2.9. Differential scanning calorimetry (DSC)

DSC experiments were performed on a STA625 thermal analyzer from Rheometric Scientific (Piscataway, New Jersey) with a constant heating rate of 10 $^{\circ}\text{C}/\text{min}$. The measurements were made in open aluminium crucibles, nitrogen was purged in ambient mode and calibration was performed using an indium standard.

3. Results and discussion

A total of 18 APIs with different functional groups including amines, amides, carboxylic acids, sulfonamides, *N*-heterocycles, amidines, esters and zwitterionic aminocarboxylates were screened (Table 1). The respective API and NaTC were physically mixed in a 1:1 molar ratio and ball-milled for 180 min. at room temperature. All API-NaTC combinations except for diflunisal-NaTC, 6-mercaptopurine-NaTC, mefenamic acid-NaTC, naproxen-NaTC and sulfathiazole-NaTC presented an amorphous halo in the XRPD pattern after milling.

Diflunisal-NaTC, 6-mercaptopurine-NaTC, mefenamic acid-NaTC, naproxen-NaTC and sulfathiazole-NaTC turned X-ray amorphous when the milling was carried out at low temperature (cryomilling). By contrast, only carbamazepine, indomethacin, sulfamerazine and sulfathiazole convert to the amorphous phase when milled without NaTC. The observation that ibuprofen and mefenamic acid can be easily amorphized on room temperature milling (ibuprofen) and cryomilling (mefenamic acid) is particularly interesting. Neat amorphous ibuprofen has a glass transition temperature T_g of $-44.10\text{ }^{\circ}\text{C}$ (Wiranidchapong et al., 2015). Generally, milling below T_g is required to achieve transformation to the amorphous form (Descamps et al., 2007). The inability of mefenamic acid to form glasses has been described in the literature (Kalra et al., 2017). According to the

classification proposed by Baird et al. (Baird et al., 2010), mefenamic acid is a class IA compound, i.e. a rapid crystallizer that crystallizes even under rapid cooling of the melt. In line with this all our attempts to amorphize mefenamic acid on its own failed.

The stabilities of the amorphous solids were assessed under ambient storage conditions and are reported in Table 1. Acyclovir-NaTC, amoxicillin-NaTC, allopurinol-NaTC, benzamidine-NaTC, carbamazepine-NaTC, diflunisal-NaTC, paracetamol-NaTC, indomethacin-NaTC, mefenamic acid-NaTC, quinine-NaTC, sulfamerazine-NaTC and sulfathiazole-NaTC remained X-ray amorphous for between one and eleven months. In the case of ciprofloxacin-NaTC, ibuprofen-NaTC, nifedipine-NaTC and norfloxacin-NaTC, Bragg peaks of the API were observed in the XRPD patterns after 22, 23, 17, and 1 d, respectively. Although not stable on a pharmaceutically relevant timescale, the stability of ibuprofen-NaTC, in particular, is still significant given that its low T_g usually makes its stabilization rather challenging (Wiranidchamong et al., 2015).

Out of the 14 APIs that were stable towards recrystallization, carbamazepine, quinine, diflunisal, indomethacin, naproxen, mefenamic acid, 6-mercaptopurine, sulfamerazine and sulfathiazole belong to BCS class II or IV, *i.e.* are poorly soluble, and the dissolution behavior of the respective API-NaTC samples was investigated (Figs. 1 and S1 – S7).

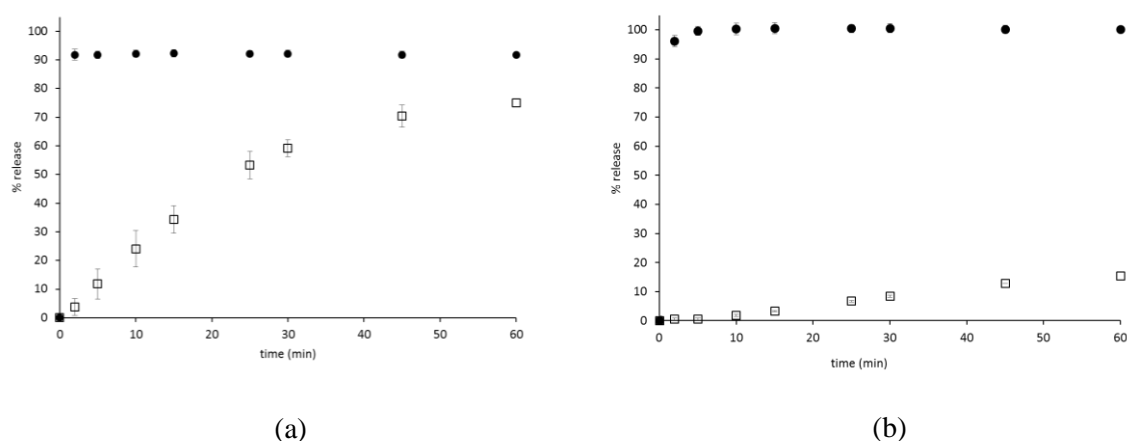


Fig. 1. Powder dissolution profiles of (a) amorphous indomethacin-NaTC and (b) mefenamic acid-NaTC (b). Phosphate buffer (pH 6.8), 37 °C. ● amorphous API-NaTC; □ crystalline API.

A significant enhancement of the dissolution rate compared to the crystalline API was observed for amorphous indomethacin-NaTC and mefenamic acid-NaTC. In fact close to 100 % release occurred almost instantaneously under sink conditions. This compares to 60 and 10 % within 30 min for crystalline indomethacin and mefenamic acid, respectively. Amorphous carbamazepine-NaTC, sulfathiazole-NaTC, diflunisal-NaTC, sulfamerazine-NaTC and quinine-NaTC also showed better dissolution behavior than the crystalline APIs. In the case of 6-mercaptopurine-NaTC and naproxen-NaTC, dissolution profiles very similar to those of crystalline 6-mercaptopurine and naproxen were recorded. For the three coamorphous systems that gave the largest dissolution advantages over the respective crystalline drug, mefenamic acid-NaTC, indomethacin-NaTC and carbamazepine-NaTC, the effect of storage on the dissolution behavior was investigated. Dissolution testing after storage in a sealed vial at room temperature for seven months showed no significant difference in the dissolution profiles compared to those of the fresh samples (Figs. S8 – S10). The dissolution behavior of co-milled indomethacin-NaTC and carbamazepine-NaTC was also compared with that of mixtures of separately milled NaTC and indomethacin/carbamazepine. XRPD confirmed that both APIs turn amorphous when milled on their own. The commercial NaTC was already X-ray amorphous. Nevertheless, the bile acid was milled prior to mixing with the amorphized API to exclude any particle size effects. Mixtures of separately milled mefenamic acid and NaTC were not studied because milling in the absence of NaTC does not lead to amorphization of the acid. Neither could amorphous mefenamic acid be obtained by melt-quenching in line with previous literature reports (Kalra et al., 2017). Freshly prepared amorphous indomethacin gently mixed with one mole equivalent amorphous NaTC using a vortex mixer gave the same dissolution profile as co-milled indomethacin-NaTC. However, after storage for 7 d, the dissolution rate decreased significantly (Fig. S11). XRPD analysis of the aged powder sample showed clear Bragg peaks of indomethacin indicating that recrystallization had occurred (data not shown). The different properties of the amorphous API in a mixture with separately milled NaTC and in a co-milled mixture were even more evident for carbamazepine-NaTC. A fresh mixture of freshly milled amorphous carbamazepine and milled NaTC showed no dissolution advantage over crystalline carbamazepine (Fig. S12). It has been reported in the literature that amorphous carbamazepine rapidly recrystallizes to the dihydrate even in the absence of buffer (Jensen et al., 2017) and our own stability monitoring of milled carbamazepine gave similar results. Taken together, the dissolution data indicate the formation of stable coamorphous systems during milling. To further confirm that NaTC in the co-milled sample does not simply

enhance the dissolution rate by acting as a surfactant, we tested the dissolution behavior in buffer containing one mole equivalent of pre-dissolved NaTC, using mefenamic acid as an example. No dissolution advantage was observed (Fig. S13).

Vibrational spectroscopy gives insight into the disruption of hydrogen bonding interactions between API molecules and into the formation of new interactions between the API and the coformer in a coamorphous system.

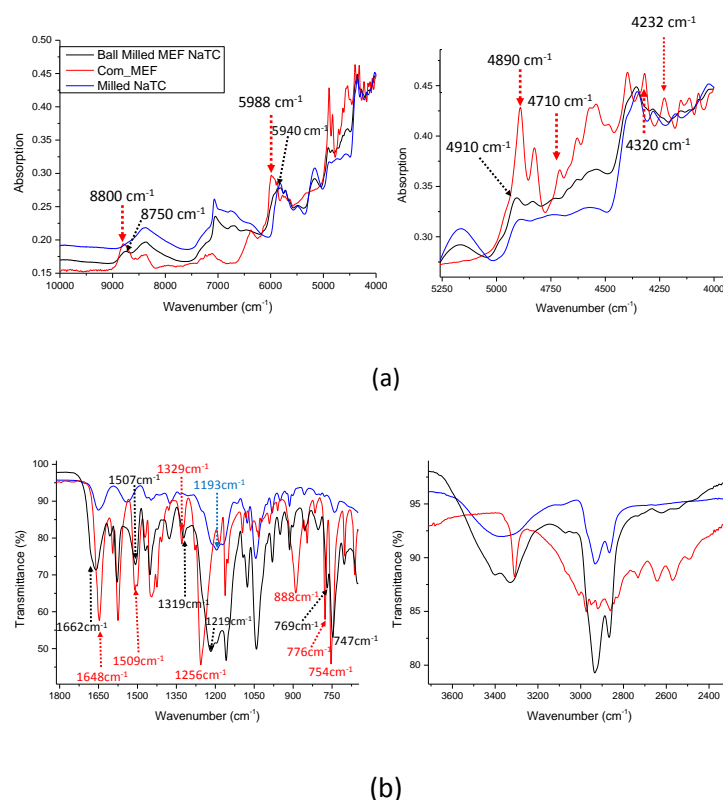


Fig. 2. (a) NIR spectra and (b) 3600 – 2400 cm^{-1} and 1800 – 750 cm^{-1} ranges of the IR spectra of mefenamic acid (commercial form, red), amorphous NaTC (blue) and a cryomilled 1:1 mixture of NaTC and mefenamic acid (black).

Fig. 2 shows the NIR and IR spectra of crystalline mefenamic acid (commercial form I), NaTC and of a 1:1 mixture of mefenamic acid and NaTC after cryomilling. Amorphization leads to the disappearance of the NIR peaks of crystalline mefenamic acid at 4232, 4320 and 4710 cm^{-1} . The peaks at 4890, 5988 and 8800 cm^{-1} shift to 4910, 5940 and 8750 cm^{-1} , respectively. In the IR spectrum, the mefenamic acid bands at 754 and 776 cm^{-1} become broader and appear at lower wavenumbers (747 and 769 cm^{-1}) after co-milling with NaTC,

while the intensity of the strong, sharp band at 888 cm^{-1} decreases. Furthermore, the band at 1256 cm^{-1} shifts to 1219 cm^{-1} and overlaps with the strong NaTC band at 1193 cm^{-1} . Other changes involve the mefenamic acid peak at 1329 cm^{-1} that moves to 1319 cm^{-1} and the split peak at $1509/1502\text{ cm}^{-1}$ that becomes a broad band centered at 1507 cm^{-1} . The C=O vibration of mefenamic acid at 1648 cm^{-1} shifts to 1662 cm^{-1} . These changes and shifts clearly indicate changes in the hydrogen bonding network of mefenamic acid on amorphization. The broadening of the IR bands is indicative of a loss of long-range order. As for the NaTC bands, the only change in the IR and NIR spectra of the co-milled sample is a slight shift of the band at 1196 cm^{-1} to a lower wavenumber (1193 cm^{-1}). Thus, there is no evidence for specific API-NaTC interactions. We further analyzed the coamorphous mefenamic acid-NaTC system by Raman microscopy (Fig. S14). Spectra taken of different particles of the co-milled sample contain spectral information from both mefenamic acid and the bile acid.

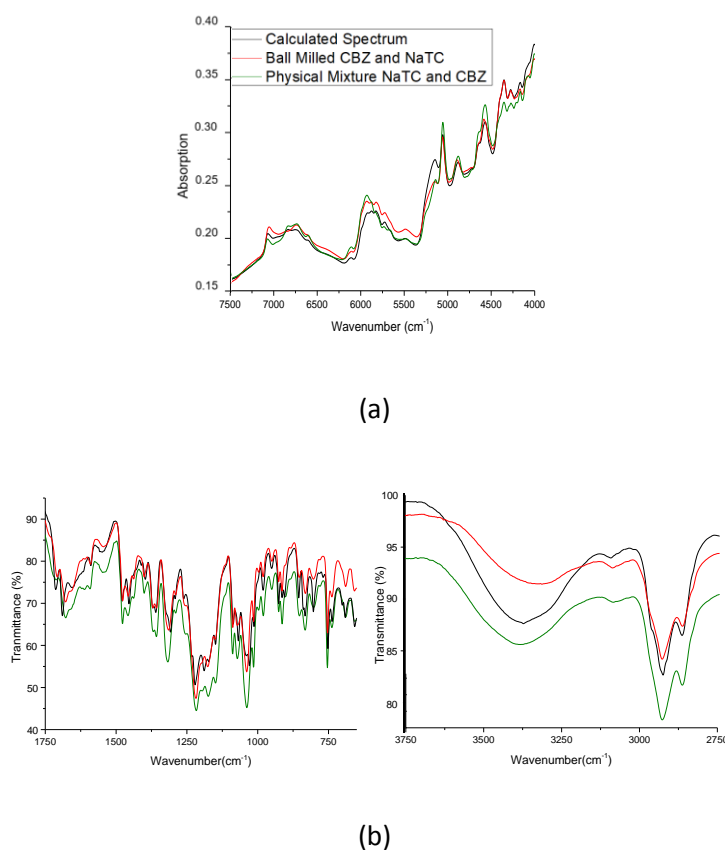


Fig. 3. (a) NIR spectra and (b) $3500 - 2750\text{ cm}^{-1}$ and $1750 - 750\text{ cm}^{-1}$ ranges of the IR spectra of co-milled carbamazepine-NaTC (red), a 1:1 mixture of separately milled carbamazepine and NaTC (green) and the calculated spectra for a physical mixture of amorphous carbamazepine and NaTC (black).

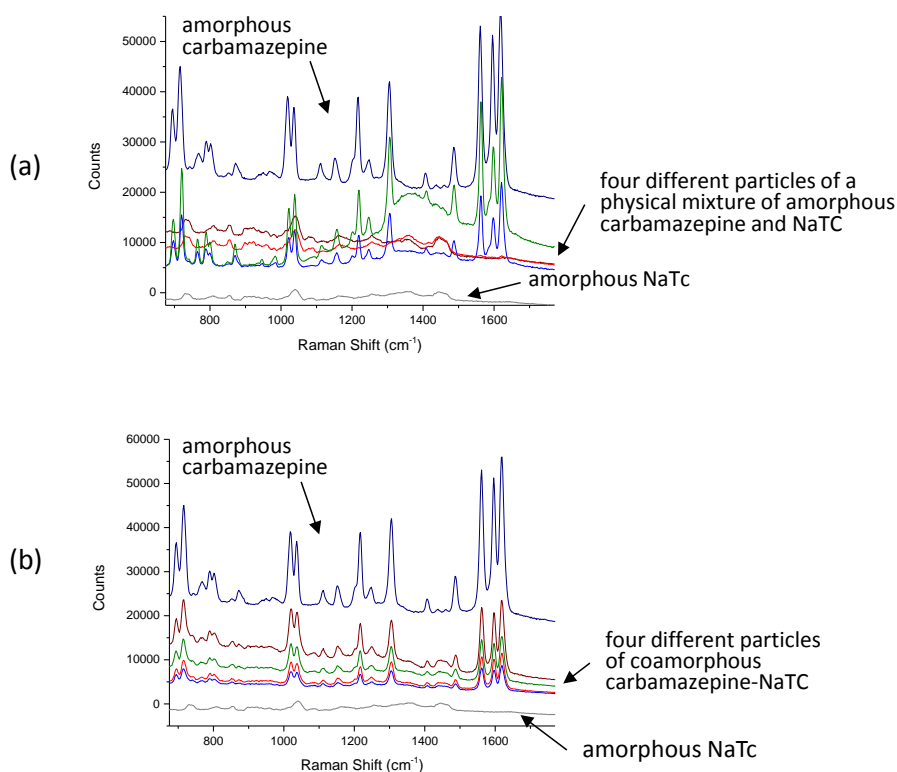


Fig. 4. Raman spectra of different particles of (a) a mixture of amorphous carbamazepine and NaTC milled separately and (b) a co-milled sample of carbamazepine-NaTC.

The NIR, IR and Raman spectra of carbamazepine-NaTC are displayed in Figs. 3, 4 and S15. Again, the appearance of broad bands is consistent with the conversion of the crystalline API into its amorphous form. The IR and NIR spectra of the co-milled sample are identical to those obtained when carbamazepine is amorphized on its own and gently mixed with amorphous NaTC in a 1:1 molar ratio. The theoretical IR and NIR spectra of a physical mixture of amorphous carbamazepine and NaTC were also calculated for comparison. The Raman spectra, on the other hand, revealed clear differences between co-milled carbamazepine-NaTC and a mixture of NaTC and carbamazepine amorphized separately. In the case of the physical mixture different particles give distinct Raman spectra featuring characteristic peaks of either the API or NaTC (Fig. 4a). By contrast, spectra taken of different particles of the co-milled sample show carbamazepine as well as bile acid bands (Fig. 4b). The laser spot size in the Raman measurements was $\leq 5 \mu\text{m}$. This is smaller than the average particle size of the co-milled sample as evident from the SEM images displayed

in Fig. 5. Thus, the increased physical stability and enhanced dissolution rate of the ball-milled carbamazepine-NaTC can be attributed to the formation of a homogeneous, intimately mixed coamorphous system.

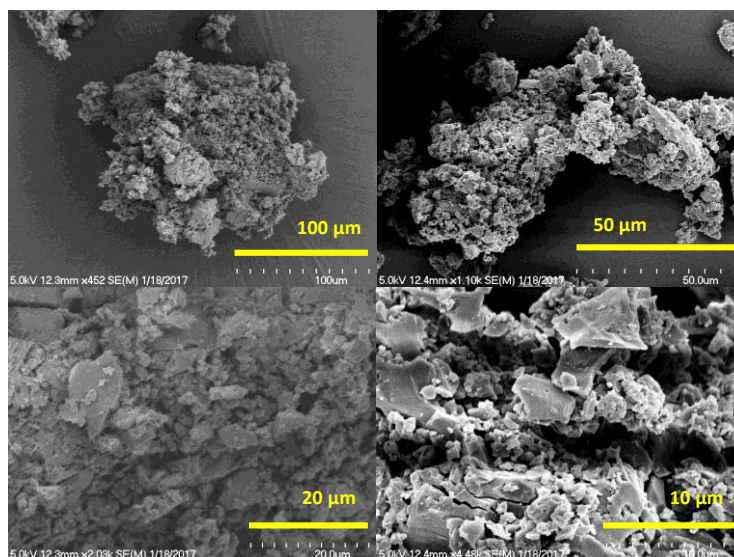


Fig. 5. SEM image of a co-milled 1:1 mixture of carbamazepine and NaTC.

A single-phase coamorphous system is characterized by a single glass transition and a T_g between the T_g s of the pure components. The Gordon-Taylor equation gives the theoretical T_g assuming ideal mixing and positive or negative deviations of the experimental T_g from the calculated value are associated with an increase or decrease in the number and/or strength of intermolecular interactions, respectively. The DSC thermogram of pure NaTC shows a very broad endotherm that encompasses the 50 to 120 °C temperature range (Fig. S16). This thermal event also dominates the thermograms of the co-milled samples so that the DSC analysis of carbamazepine-NaTC (and of all other NaTC-API systems) is inconclusive.

Like carbamazepine-NaTC, co-milled indomethacin-NaTC gives broad IR bands. Again, the NIR and IR spectra (Fig. S17) are indistinguishable from those of a physical mixture of amorphous indomethacin and amorphous NaTC, while Raman microscopy (Fig. S18) distinguishes between coamorphized and physically mixed amorphous indomethacin and NaTC. IR and NIR spectroscopy are bulk techniques that do not differentiate between

molecular level mixing and the presence of API and coformer domains. Nevertheless, based on the spectral analysis of co-milled samples and physical mixtures of the amorphous components, specific hydrogen bonding interactions between NaTC and carbamazepine/indomethacin can be ruled out. On the other hand, the significantly increased physical stabilities during storage and in the case of carbamazepine-NaTC also during dissolution testing are indirect evidence for a well-mixed coamorphous system. NaTC belongs to the group of molecules with an awkward molecular shape whose crystallization is likely to be hampered by packing difficulties. Crystal structures are available for two hydrates/ solvates of NaTC. CSD code KORZUM has the formula $\text{NaTC} \cdot 2.5\text{H}_2\text{O}$ and CSD Code YEGNON has the formula $2(\text{NaTc}) \cdot 11.5\text{H}_2\text{O} \cdot \text{acetone}$ (Campanelli et al., 1991, D'Alagni et al., 1994). The packing indices for these structures are 61.0 and 60.2% respectively. Kitaigorodskii was the first to suggest that organic compounds can pack efficiently with packing indices close to the 74% value exhibited by close packed spheres (Kitaigorodskii, 1961) and structure surveys have supported this idea (Dunitz et al., 2000). The relatively low packing indices of the NaTC structures are typical of steroid and other molecules which have an awkward shape and can be difficult to crystallize from solution without solvent molecules in the lattice. Solvent free crystals for some steroids can be grown by sublimation but often contain voids (Karpinska et al., 2011). This packing difficulty combined with a high hydrogen bonding capacity (OH, C=O, amide-NH, sulfonyl-O) makes NaTC suitable for the formation of coamorphous API-NaTC systems. It is also likely that it is the presence of such a range of hydrogen bonding opportunities and the non-crystalline nature of the API-NaTC systems that leads to the absence of evidence for *specific* interactions in the IR data.

The question arises as to why the physical stabilities of the co-amorphous systems of nifedipine, ibuprofen, ciprofloxacin and norfloxacin are so much lower than that of the other NaTC/API combinations. For polymeric ASDs of telmisartan a correlation between the physical stability and the Flory-Huggins solubility parameter was found (Dukeck et al., 2013). On the other hand, Taylor and coworkers showed that amorphous nifedipine has a lower physical stability than felodipine, both alone and in ASDs, although the two related compounds have a very similar T_g and molecular mobility (Marsac et al., 2006). They pointed out that the difference between the free energy of the amorphous phase and the free energy of the crystalline phase as well as the kinetics of crystallization have to be considered. It was demonstrated that nifedipine has a larger enthalpic driving force for recrystallization

than felodipine and concluded that the physical stability of ASDs is not only determined by the properties of the amorphous phase but also depends on the properties of the crystalline API. In other words, similar to ASDs, the relative stabilities of coamorphous NaTC/API systems may be expected to follow the crystallization tendencies of the pure APIs. Ibuprofen has already been discussed above. The crystal structures of ciprofloxacin hexahydrate (Turel et al., 1997) and norfloxacin (Barbas et al., 2007) revealed that both compounds exist in the zwitterionic form so that the crystal lattice is stabilized by strong charge-assisted H bonds.

4. Conclusions

A wide range of APIs, including poor glass formers such as mefenamic acid, can be amorphized by co-milling with one mole equivalent NaTC. The majority of the co-milled API-NaTC systems are physically stable under ambient storage conditions. Besides an enhanced solid-state stability, amorphous carbamazepine-NaTC, indomethacin-NaTC and mefenamic acid-NaTC also display a significant dissolution advantage over the crystalline drugs, even after storage for seven months. The dissolution, IR, NIR and Raman data of the three API-NaTC systems that were studied in greater detail and compared with the respective physical mixtures of the amorphous API and NaTC are consistent with the milling-induced formation of homogenous, intimately mixed coamorphous systems.

Because of its awkward molecular shape and poor propensity to crystallize, NaTC appears to be well-suited to prevent the rearrangement of the API molecules and thus the phase separation of the coamorphous systems. This is combined with a high hydrogen bonding capacity (OH, C=O, amide-NH, sulfonyl-O). The presence of three OH groups allows for the coexistence of different, but similar hydrogen bonded arrangements in the coamorphous API-NaTC systems. In summary, NaTC appears to be an ideal and versatile coformer for coamorphization as it is a poor crystallizer with packing difficulties and a high hydrogen bonding capacity that – rather than forming specific interactions with an API – allows for a variety of different hydrogen-bonded arrangements. This leads to stable coamorphous systems with a diverse range of APIs.

Acknowledgements

This work was supported by Science Foundation Ireland under Grant No. [12/RC/2275] as part of the Synthesis and Solid State Pharmaceutical Centre (SSPC).

Appendix-A. Supplementary data

Additional experimental details; additional dissolution profiles; near infrared, infrared and Raman spectra.

References

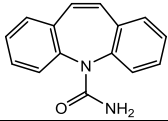
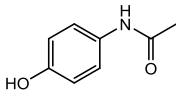
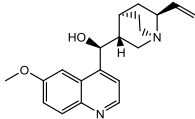
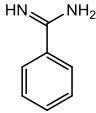
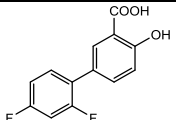
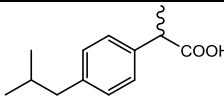
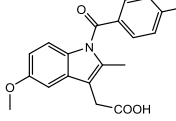
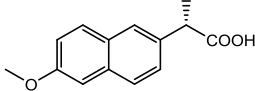
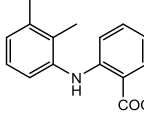
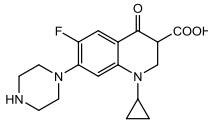
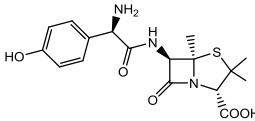
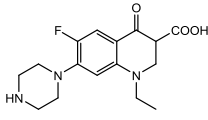
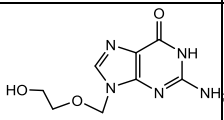
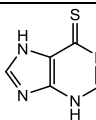
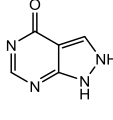
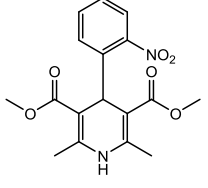
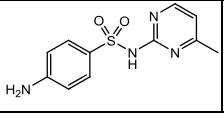
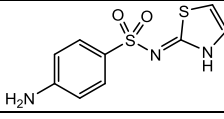
- Ali, A.M.A., Ali, A.A., Maghrabi, I.A., 2015. Clozapine-carboxylic acid plasticized coamorphous dispersions: preparation, characterization and solution stability evaluation. *Acta Pharm.* 65, 133–146.
- Allesø, M., Chieng, N., Rehder, S., Rantanen, J., Rades, T., Aaltonen, J., 2009. Enhanced dissolution rate and synchronized release of drugs in binary systems through formulation: amorphous naproxen-cimetidine mixtures prepared by mechanical activation. *J. Control. Release* 136, 45–53.
- Baird, J.A., Van Eerdenbrugh, B., Taylor, L.S., 2010. A classification system to assess the crystallization tendency of organic molecules from undercooled melts. *J. Pharm. Sci.* 99, 3787–3806.
- Campanelli, A. R., Candeloro De Sanctis, S., D'Archivio, A. A., Giglio, E., Scaramuzza, L., 1991. Crystal structures of bile salts: Sodium taurocholate. *J. Inclusion Phenom.* 11, 247–256.
- Chauhan, B., Shimpi, S., Paradkar, A., 2005. Preparation and evaluation of glibenclamide-polyglycolized glycerides solid dispersions with silicon dioxide by spray drying technique. *Eur. J. Pharm. Sci.* 26, 219–230.
- Chieng, N., Aaltonen, J., Saville, D., Rades, T., 2009. Physical characterization and stability of amorphous indomethacin and ranitidine hydrochloride binary systems prepared by mechanical activation. *Eur. J. Pharm. Biopharm.* 71, 47–54.
- Craye, G., Löbmann, K., Grohgan, H., Rades, T., Laitinen, R., 2015. Characterization of amorphous and co-amorphous simvastatin formulations prepared by spray drying. *Molecules* 20, 21532–21548.
- D'Alagni, M., Galantini, L., Giglio, E., Gavuzzo, E., Scaramuzza, L., 1994. Micellar aggregates of sodium glycocholate and sodium taurocholate and their interaction complexes with bilirubin-IX α . Structural models and crystal structure. *J. Chem. Soc., Faraday Trans.* 90, 1523–1532.

- Descamps, M., Willart, J., Dudognon, E., Caron, V., 2007. Transformation of pharmaceutical compounds upon milling and comilling: the role of T_g . *J. Pharm. Sci.* 96, 1398–1407.
- Dukeck, R., Sieger, P., Karmwar, P., 2013. Investigation and correlation of physical stability, dissolution behaviour and interaction parameter of amorphous solid dispersions of telmisartan: A drug development perspective. *Eur. J. Pharm. Sci.* 49, 723–731.
- Dunitz, J. D., Filippini, G., Gavezzotti, A., 2000. A Statistical study of density and packing variations among crystalline isomers, *Tetrahedron* 56, 6595–6601.
- Gao, Y., Liao, J., Qi, X., Zhang, J., 2013. Coamorphous repaglinide-saccharin with enhanced dissolution. *Int. J. Pharm.* 450, 290–295.
- Gniado, K., Löbmann, K., Rades, T., Erxleben, A., 2016. The influence of co-formers on the dissolution rates of co-amorphous sulfamerazine/excipient systems. *Int. J. Pharm.* 504, 20–26.
- Grohgan, H., Priemel, P.A., Löbmann, K., Nielsen, L.H., Laitinen, R., Mullertz, A., Van den Mooter, G., Rades, T., 2014. Refining stability and dissolution rate of amorphous drug formulations. *Exp. Opin. Drug Deliv.* 11, 977–989.
- Guo, Y., Shalaev, E., Smith, S., 2013. Physical stability of pharmaceutical formulations: solid-state characterization of amorphous dispersions. *Trends Anal. Chem.* 49, 137–144.
- Han, Y., Pan, Y., Lv, J., Guo, W., Wang, J., 2016. Powder grinding preparation of coamorphous β -azelnidipine and maleic acid combination: molecular interactions and physicochemical properties. *Powder Technol.* 291, 110–120.
- Hoppu, P., Jouppila, K., Rantanen, J., Schantz, S., Juppo, A.M., 2007. Characterisation of blends of paracetamol and citric acid. *J. Pharm. Pharmacol.* 59, 373–381.
- Hoppu, P., Hietala, S., Schantz, S., Juppo, A.M., 2009. Rheology and molecular mobility of amorphous blends of citric acid and paracetamol. *Eur. J. Pharm. Biopharm.* 71, 55–63.
- Hu, Y., Gniado, K., Erxleben, A., McArdle, P., 2014. Mechanochemical reaction of sulfathiazole with carboxylic acids: formation of a cocrystal, a salt, and coamorphous solids. *Cryst. Growth Des.* 14, 803–813.
- Huang, Y., Zhang, Q., Wang, J.-R., Lin, K.-L., Mei, X., 2016. Amino acids as coamorphous excipients for tackling the poor aqueous solubility of valsartan. *Pharm. Dev. Technol.* 1–8.

- Jensen, K.T., Löbmann, K., Rades, T., Grohgan, H., 2014. Improving co-amorphous drug formulations by the addition of the highly water soluble amino acid, proline. *Pharmaceutics* 6, 416–435.
- Jensen, K.T., Larsen, F.H., Cornett, C., Löbmann, K., Grohgan, H., Rades, T., 2015. Formation mechanism of coamorphous drug–amino acid mixtures. *Mol. Pharmaceutics* 12, 2484–2492.
- Jensen, K.T., Blaabjerg, L.I., Lenz, E., Bohr, A., Grohgan, H., Kleinebudde, P., Rades, T., Löbmann, K., 2016. Preparation and characterization of spray-dried coamorphous drug–amino acid salts. *J. Pharm. Pharmacol.* 68, 615–624.
- Jensen, L.G., Skautrup, F.B., Müllertz, A., Abrahamsson, B., Rades, T., Priemel, P.A., 2017. Amorphous is not always better - A dissolution study on solid state forms of carbamazepine. *Int. J. Pharm.* 522, 74–79.
- Kalra, A., Tishmack, P., Lubach, J.W., Munson, E.J., Taylor, L.S., Byrn, S.R., Li, T., 2017. *Mol. Pharmaceutics* 14, 2126–2137.
- Karpinska, J., Erxleben, A., McArdle, P., 2011. 17 β -hydroxy-17 α -methylandro-stano[3,2-c]-pyrazole, Stanazolol: The crystal structures of polymorphs 1 and 2 and ten solvates. *Cryst. Growth Des.* 11, 2829–2838.
- Kaushal, A.M., Gupta, P., Bansal, A.K., 2004. Amorphous drug delivery systems: molecular aspects, design, and performance. *Crit. Rev. Ther. Drug Carrier Syst.* 21, 1–62.
- Kitaigorodskii, A. I., *Organic Chemical Crystallography*. ed.; Consultant's Bureau: New York: 1961.
- Laitinen, R., Löbmann, K., Grohgan, H., Strachan, C., Rades, T., 2014. Amino acids as co-amorphous excipients for simvastatin and glibenclamide: physical properties and stability. *Mol. Pharmaceutics* 11, 2381–2389.
- Lenz, E., Jensen, K.T., Blaabjerg, L.I., Knop, K., Grohgan, H., Löbmann, K., Rades, T., Kleinebudde, P., 2015. Solid-state properties and dissolution behaviour of tablets containing co-amorphous indomethacin–arginine. *Eur. J. Pharm. Biopharm.* 96, 44–52.
- Löbmann, K., Laitinen, R., Grohgan, H., Gordon, K.C., Strachan, C., Rades, T., 2011. Coamorphous drug systems: enhanced physical stability and dissolution rate of indomethacin and naproxen. *Mol. Pharmaceutics* 8, 1919–1928.
- Löbmann, K., Strachan, C., Grohgan, H., Rades, T., Korhonen, O., Laitinen, R., 2012. Co-amorphous simvastatin and glipizide combinations show improved physical stability without evidence of intermolecular interactions. *Eur. J. Pharm. Biopharm.* 81, 159–169.

- Löbmann, K., Grohgan, H., Laitinen, R., Strachan, C., Rades, T., 2013. Amino acids as co-amorphous stabilizers for poorly water soluble drugs - Part 1: Preparation, stability and dissolution enhancement. *Eur. J. Pharm. Biopharm.* 85, 873–881.
- Lu, Q., Zografi, G., 1998. Phase behavior of binary and ternary amorphous mixtures containing indomethacin, citric acid and PVP. *Pharm. Res.* 15, 1202–1206.
- Marsac, P.J., Konno, H., Taylor, L.S., 2006. A comparison of the physical stability of amorphous felodipine and nifedipine systems. *Pharm. Res.* 23, 2306–2316.
- Masuda, T., Yoshihashi, Y., Yonemochi, E., Fujii, K., Uekusa, H., Terada, K., 2012. Cocrystallization and amorphization induced by drug–excipient interaction improves the physical properties of acyclovir. *Int. J. Pharm.* 422, 160–169.
- Barbas, R., Prohens, R., Puigjaner, C., 2007. A new polymorph of norfloxacin. Complete characterization and relative stability of its trimorphic system. *J. Therm. Anal. Calorim.* 89, 687–692.
- Shayanfar, A., Ghavimi, H., Hamishekar, H., Jouyban, A., 2013. Coamorphous atorvastatin calcium to improve its physicochemical and pharmacokinetic properties. *J. Pharm. Pharm. Sci.* 16, 577–587.
- Teja, S.B., Patil, S.P., Shete, G., Patel, S., Bansal, A.K., 2013. Drug-excipient behavior in polymeric amorphous solid dispersions. *J. Excip. Food Chem.* 4, 70–94.
- Turel, I., Bukoveca, P., Quirós, M., 1997. Crystal structure of ciprofloxacin hexahydrate and its characterization. *Int. J. Pharm.* 152, 59–65.
- Wiranidchamong, C., Ruangpayungsak, N., Suwattanasuk, P., Shuwisitkul, D., Tanvichien, S., 2015. Plasticizing effect of ibuprofen induced an alteration of drug released from Kollidon SR matrices produced by direct compression. *Drug Dev. Ind. Pharm.* 41, 1037–1046.
- Won, D.-H., Kim, M.S., Lee, S., Park, J.S., Hwang, S.J., 2005. Improved physicochemical characteristics of felodipine solid dispersion particles by supercritical anti-solvent precipitation process. *Int. J. Pharm.* 301, 199–208.
- Yamura, S., Momose, Y., Takahashi, K., Nagatani, S., 1996. Solid-state interaction between cimetidine and naproxen. *Drug Stab.* 1, 173–178.
- Yamura, S., Gotoh, H., Sakamoto, Y., Momose, Y., 2000. Physicochemical properties of amorphous precipitates of cimetidine-indomethacin in binary system. *Eur. J. Pharm. Biopharm.* 49, 259–265.

Table 1. Chemical structures of the APIs used in this study and stabilities of coamorphous API-NaTC systems (sealed vial, ambient temperature and relative humidity)

API		Stability	API		Stability
<i>Amides</i>					
Carbamazepine		12 months	Paracetamol		6 months
<i>Amines</i>			<i>Amidines</i>		
Quinine		>11 months	Benzamidine		5 months
<i>Carboxylic acids</i>					
Diffunisal		>2 months	Ibuprofen		3 weeks
Indomethacin		>11 months	Naproxen		>2 months
Mefenamic acid		>11 months			
<i>Aminocarboxylic acids</i>					
Ciprofloxacin		3 weeks	Amoxicillin		>11 months
Norfloxacin		1 day			
<i>Purines</i>					
Acyclovir		6 months	6-mercaptopurine		2 months
Allopurinol		>4 months			
<i>Esters</i>					
Nifedipine		17 days			
<i>Sulfonamides</i>					
Sulfamerazine		12 months	sulfathiazole		3 months

--	--	--	--	--	--